Acta Pharmacologica Sinica

www.nature.com/aps

ARTICLE

Macrod1 suppresses diabetic cardiomyopathy via regulating PARP1-NAD$^+$-SIRT3 pathway

Yu-ting Liu[1,2], Hong-liang Qiu[1,2], Hong-xia Xia[1,2], Yi-zhou Feng[1,2], Jiang-yang Deng[1,2], Yuan Yuan[1,2], Da Ke[1,2], Heng Zhou[1,2], Yan Che[1,2]✉ and Qi-zhu Tang[1,2]✉

Diabetic cardiomyopathy (DCM), one of the most serious long-term consequences of diabetes, is closely associated with oxidative stress, inflammation and apoptosis in the heart. MACRO domain containing 1 (Macrod1) is an ADP-ribosylhydrolase 1 that is highly enriched in mitochondria, participating in the pathogenesis of cardiovascular diseases. In this study, we investigated the role of Macrod1 in DCM. A mice model was established by feeding a high-fat diet (HFD) and intraperitoneal injection of streptozotocin (STZ). We showed that Macrod1 expression levels were significantly downregulated in cardiac tissue of DCM mice. Reduced expression of Macrod1 was also observed in neonatal rat cardiomyocytes (NRCMs) treated with palmitic acid (PA, 400 μM) in vitro. Knockout of Macrod1 in DCM mice not only worsened glycemic control, but also aggravated cardiac remodeling, mitochondrial dysfunction, NAD$^+$ consumption and oxidative stress, whereas cardiac-specific overexpression of Macrod1 partially reversed these pathological processes. In PA-treated NRCMs, overexpression of Macrod1 significantly inhibited PARP1 expression and restored NAD$^+$ levels, activating SIRT3 to resist oxidative stress. Supplementation with the NAD$^+$ precursor Niacin (50 μM) alleviated oxidative stress in PA-stimulated cardiomyocytes. We revealed that Macrod1 reduced NAD$^+$ consumption by inhibiting PARP1 expression, thereby activating SIRT3 and anti-oxidative stress signaling. This study identifies Macrod1 as a novel target for DCM treatment. Targeting the PARP1-NAD$^+$-SIRT3 axis may open a novel avenue to development of new intervention strategies in DCM.

Keywords: diabetic cardiomyopathy; Macrod1; PARP1; NAD$^+$; SIRT3; oxidative stress

Acta Pharmacologica Sinica (2024) 0:1–14; https://doi.org/10.1038/s41401-024-01247-2

INTRODUCTION

Diabetes has become one of the most prevalent chronic diseases in the world, threatening the security of the global population and causing serious health issues [1]. Diabetic cardiomyopathy (DCM) is one of the serious complications of diabetes that can eventually develop into heart failure [2]. Compared with complex mechanisms such as inflammation, mitochondrial oxidative stress damage occurs throughout the process of DCM, and reducing oxidative stress can significantly improve DCM prognosis [3]. Mitochondrial structure and redox homeostasis play central roles during DCM progression [4, 5]. Currently, diabetes-induced cardiac dysfunction is mostly treated by controlling risk factors, reducing microvascular damage, and improving the prognosis, and there is a lack of effective treatment options. Therefore, it is urgent to discover promising therapeutic targets for diabetic cardiomyopathy.

MACRO domain containing 1 (Macrod1), an ADP-ribosylhydrolase 1, also known as leukemia-associated protein 16 (LRP16), activates ADP-ribosylaspartate hydrolase and glutamate deacetylase, and participates in ADP-ribosylation modification [6, 7]. As a cytoplasmic protein, Macrod1 is also predominantly expressed in energy-consuming organs such as the heart and skeletal muscles. Consequently, it is highly enriched in mitochondria, mediating the occurrence of cardiovascular diseases [8–10]. Previous studies have demonstrated that Macrod1 activates the NF-κB signaling pathway through interaction with PARP1 and IKKγ to mitigate cell death caused by DNA double-strand break damage [11]. As a post-translational protein modification (PTM), ADP-ribosylation uses NAD$^+$ to join ADP-ribose fragments to deplete mitochondrial nicotinamide adenine nucleotide (NAD$^+$) levels, and may impair mitochondrial energy status under pathological stress conditions. Recent studies have highlighted the role of PARP inhibitors in myocardial oxidative stress injury and apoptosis [12, 13]. Therefore, Macrod1 might potentially be linked to mitochondrial energy metabolism and redox homeostasis through ADP ribosylation in DCM. Identifying Macrod1's role and underlying mechanism will be of substantial significance in DCM treatment.

Sirtuins are a class of seven congeners consisting of NAD$^+$-dependent histone deacetylases (HDACs). Sirtuin3 (SIRT3), as a member of the SIRT family, is highly expressed in energy-consuming tissue. According to previous studies, SIRT3 plays a crucial role in mitochondrial dysfunction and redox homeostasis [14]. Furthermore, SIRT3 exhibited a protective effect on cardiac hypertrophy and ventricular remodeling in mice induced by transverse aortic constriction (TAC) [15]. Previous studies have shown that SIRT3 knockout mice have significantly shorter lifespans than wild-type mice, with progressive age-related cardiac dysfunction characterized by myocardial hypertrophy and fibrosis

[1]Department of Cardiology, Renmin Hospital of Wuhan University, Wuhan 430060, China and [2]Hubei Key Laboratory of Metabolic and Chronic Diseases, Wuhan 430060, China
Correspondence: Yan Che (cheyan@whu.edu.cn) or Qi-zhu Tang (qztang@whu.edu.cn)
These authors contributed equally: Yu-ting Liu, Hong-liang Qiu.

Received: 30 November 2023 Accepted: 19 February 2024
Published online: 08 March 2024

[16]. A recent study has shown that SIRT3 contributes to regulating apoptosis in cardiomyocytes and reduces cardiac inflammation [17]. Among its various biological functions, SIRT3 is crucial for energy homeostasis, cardiac remodeling, and heart failure.

Several complex molecular mechanisms and pathophysiological activities have been implicated in diabetic cardiomyopathy. Recently, we have made some progress in the exploration of the mechanism of diabetes [18–20]. In this study, we investigated the role and mechanism of Macrod1 in high-fat diet (HFD) and streptozotocin (STZ)-induced diabetic cardiomyopathy. We found that Macrod1 expression is downregulated in cardiac tissue and cardiomyocytes in DCM, and knocking down Macrod1 causes an increase in PARP1 and a decrease in SIRT3 expression. Mechanistically, this study identified that Macrod1 alleviates heart damage and oxidative stress in diabetic cardiomyopathy via the PARP1-NAD^+-SIRT3 axis, suggesting that targeting Macrod1 is a potential therapeutic strategy for DCM.

MATERIALS AND METHODS

Animals and treatments

Macrod1 knockout mice (Macrod1-KO) were constructed by Cyagen Bioscience Inc. (Suzhou, China), and C57BL/6 wild type mice (C57) were purchased from Chinese Academy of Medical Sciences (Beijing, China). All mice were maintained under specific-pathogen-free (SPF) restriction (temperature: 20–25 °C, humidity: 50 ± 5%) and complied with the Guide for the Care and Use of Laboratory Animals (NIH Publication, revised 2011). The subjects were healthy male mice aged 8–10 weeks old with a weight of 23–25 g. Experimentation with animals was approved by the Animal Care and Use Committee of Renmin Hospital of Wuhan University (Approval Number: WDRM-20220906B).

We constructed a diabetic cardiomyopathy (DCM) model after 16 weeks of feeding on a high-fat diet (HFD, Research Diets: 60.3% kcal fat and 1.5% kcal cholesterol) and intraperitoneally injected streptozocin (STZ, Sigma-Aldrich, St Louis, MO, USA) in a dose of 30 mg/kg every day for 7 consecutive days. The control group of mice was fed a normal chow diet and received an intraperitoneal injection with citrate–phosphate buffer. A diabetic mouse model was successfully established as fasting blood glucose levels averaged 16.6 mmol/L. The 8-week-old male mice of C57 and Macrod1-KO were randomly divided into 4 groups ($n = 6$ per group): C57+Sham group, Macrod1-KO+Sham group, C57 mice with diabetic cardiomyopathy group (C57 + DCM), and Macrod1-KO mice with diabetic cardiomyopathy group (Macrod1-KO + DCM). Mouse hearts and serum samples obtained to be analyzed for pathology and biochemistry, and fasting blood glucose, body weight (BW), and heart weight/tibial length (HW/TL) were measured in each group of mice.

Adeno-associated virus serotype 9 (AAV9) vector carrying the *Macrod1* gene (AAV9- *Macrod1*) with a cTnT promoter was used to overexpress MACROD1 specific in the heart, and AAV9-NC was used as control (DesignGene, Shanghai, China). Viral particles (1×10^{12} vector genomes per animal in a total of 100 μL PBS) were administered to mice through tail injection. Four weeks after AAV9 infection, the mice constructed a diabetic cardiomyopathy model grouped as follows: AAV9-NC, AAV9-*Macrod1*, AAV9-NC + DCM, and AAV9-*Macrod1* + DCM.

Echocardiography

Based on our previous study, transthoracic echocardiography was performed using a linear array ultrasound transducer with a probe capable of 30-MHz (Vevo 3100 system Visual Sonics) [21]. We detected the heart function of each group of mice by small animal sonicator, including left ventricular ejection fraction (LVEF), left ventricular fraction shortening (LVFS) and heart rate (HR) at the experimental endpoint. Simultaneously, we measured long-axis left ventricular endocardial strain by speckle tracking echocardiography. VevoStrain analysis software was used to analyze longitudinal and radial strains and examine Global longitudinal strain (GLS), LV endocardial radial strain and LV endocardial maximum opposing wall delay in long axis.

Intraperitoneal glucose tolerance test

Following a 12-h fast, mice undergo an intraperitoneal glucose tolerance test (OGTT). In the glucose loading procedure, mice receive 1.0 mg/kg glucose injections. The amount of glucose in their blood is measured during the first 15 min after injection and the following 30 min, 60 min and 120 min thereafter (Sanesu Sano, Changsha, China).

Histological staining

Hematoxylin and eosin (H&E) staining was used to observe myocardial morphological changes in mice. Following the manufacturer's instructions (Beyotime, Shanghai, China), terminal deoxynucleotidyl transferase dUTP nick-end labeling (TUNEL) staining was used to detect apoptosis in mice hearts. Afterward, images were captured with an Olympus DX51 fluorescence microscope and analyzed with Image-Pro Plus version 6.0 (Media Cybernetics, MD, USA).

Mitochondrial morphology and function assessment

Terminal mouse myocardial tissue from both experimental and control groups was isolated, and the apical tissue was immersed in the electron microscope fixative at 4 °C. At the Electron Microscopy Center of Renmin Hospital of Wuhan University, mitochondria morphology, number, arrangement, and structural changes were examined by a transmission electron microscope (TM-3000; Hitachi Ltd., Tokyo, Japan). We also measured the ATP production rate to assess the energetic status of Macrod1-KO mice at baseline according to our previous study method [20].

Immunofluorescence

To further examine Macrod1 and PARP1 expression in mice's heart tissues, immunofluorescence staining is required. Based on our previous experimental instructions [22], the paraffin sections were incubated overnight with primary antibodies of different species, including Macrod1 or PARP1 and α-actinin. On the second day, the heart sections were incubated secondary antibodies to detect fluorescence, including Alexa Fluor 488 Goat Anti-Mice/Rabbit IgG and Alexa Fluor 568 Goat Anti-Mice/Rabbit IgG. In the nucleus, 4',6-diamido-2-phenylindole (DAPI) (Invitrogen, S36939) is eventually substituted for the nucleus.

Immunohistochemistry

Following our previous experimental guidelines [23], mouse heart paraffin sections were incubated with 4-hydroxynonenal (4-HNE) antibody overnight at 4 °C. After removing the primary antibody from the sections, the sections were incubated with anti-rabbit/mouse EnVision™ + /horseradish peroxidase reagent at 37 °C for 1 h, and reacted with 3,3′-diaminobenzidine to detect positivity (Gene Technology, Shanghai, China; GK600705). After counterstaining with hematoxylin, the sections were dehydrated and mounted for photographic examination. Photographs were taken with Nikon H550L (Tokyo, Japan) and analyzed in Image-Pro Plus (version 6.0).

Cell culture and treatment

After sterilization and sacrifice of newborn Sprague– Dawley rats at 1–2 days of age, the heart ventricular tissue was subdivided into 1–3 mm fragments, digested by 0.125% pancreatin-EDTA (2520-072, Gibco, USA) for 15 min and repeated several times, and preserved in Dulbecco's modified Eagle's medium/F-12 (C11330500BT, Gibco, USA) containing 20% fetal bovine serum (FBS, 10099-141, Gibco, USA). Then we obtained Neonatal Rat Cardiomyocytes (NRCMs) and Neonatal Rat Cardiac Fibroblasts

(NRCFs). Endothelial cells (ECs) bind specifically to CD31 beads for isolation and extraction. After extensive washing, the cells were cultured on culture dishes precoated with 2% gelatin (Sigma, Oakville, ON, Canada). After isolating NRCMs cells, cellular NAD^+ levels are exogenously supplemented by supplementing the NAD^+ precursor Niacin (NA, MCE, HY-B0143) in the NRCMs culture medium. NA was dissolved in PBS and added to NRCMs to a final concentration of 50 μM.

Adenovirus transfection
Transfection of NRCMs with adenovirus Macrod1 (Ad-*Macrod1*) constructed a model of Macrod1 overexpression cardiomyocyte, palmitic acid (PA, 400 μM, MCE, HY-N0830) produced a model of DCM in vitro, and BSA and Ad-NC formed a control group, and then grouped as follows: BSA+Ad-NC, BSA+Ad-*Macrod1*, PA+Ad-NC and PA+Ad-*Macrod1*.

SiRNA transfection
After 48 h of cardiomyocytes were cultured in 6-well or 24-well plates and PA treated appropriately, the DCM model was constructed in vivo. We transfected 100 nmol/L SIRT3 small interfering RNA (si-SIRT3) or a control nonspecific siRNA (Santa Cruz) for 4 h into NRCMs using Lipofectamine® 6000 transfection reagent to the above four groups (BSA+Ad-NC, BSA+Ad-*Macrod1*, PA+Ad-NC and PA+Ad-*Macrod1*).

NAD^+ measurement
Following hearts and NRCMs collection, lysate is added to the cells, along with a working solution of dehydrogenase. To obtain total NAD^+ and NADH, the suspension is incubated for 10 min at 37 °C. The NAD^+ or NADH test kit (Beyotime, S0175, Shanghai, China) was used to determine the level of NAD^+ or NADH in hearts and NRCMs.

JC-1 staining
To measure mitochondrial membrane potential in NRCMs, we used the JC-1 fluorescent probe (Beyotime, Shanghai, China). NRCMs were grouped according to Macrod1 overexpression or knockdown in the same manner as above. Following the manufacturer's instructions, they were incubated in JC-1 working solution and washed in JC-1 buffer solution. The imagery was captured using an Olympus fluorescence microscope DX51 (Tokyo, Japan), and an analysis of the ratio of red/green fluorescence intensity was performed to assess mitochondrial damage.

Enzyme-linked immunosorbent assay (ELISA)
Mice blood was collected from orbital veins in each group and serum was obtained after centrifuged at 10,000 × *g* for 5 min. An automatic biochemical analyzer (ADVIA® 2400, Siemens Ltd., China) was used to detect the expression levels of cardiac injury markers LDH and CK-MB in serum, and inflammatory factors IL-1β, IL-6 and TNF-α.

Oxidative stress assays
ROS levels were assessed with 2',7'-dichlorofluorescin diacetate (DCFH-DA) staining in NRCMs and Dihydroethidium (DHE) staining in heart sections. DAPI was then used to counterstain the nucleus. After that, all images were taken with an Olympus DX51 fluorescence microscope and analyzed with Image-Pro Plus version 6.0 (Media Cybernetics, Maryland, USA). In accordance with our previous study [24], the thiobarbituric acid reactive substances (TBARS) assay kit (Nanjing, China) was used to assess myocardial and cardiomyocyte MDA levels or superoxide dismutase (SOD) activities in each group.

Western immunoblotting
Based on our previous experimental instructions [25], we used RIPA lysis buffer (Servicebio, Wuhan, China) for protein extraction and BCA kit (Servicebio, Wuhan, China) for quantification. The protein undergoes electrophoresis with polyacrylamide gel (SDS-PAGE) and is transferred to polyvinylidene difluoride (PVDF) membranes, followed by blocking with 5% skim milk and washing in PBS. PVDF membranes were incubated with the primary antibody separately at 4 °C overnight. The next day, the secondary antibody was incubated for 1 h at room temperature. Finally, the level of relevant proteins was measured using the Odyssey Infrared Imaging System (LI-COR Biosciences, Lincoln, NE, USA) and analyzed through Image Lab software (v3.0; Bio-Rad Laboratories, Inc.). Supplementary Table S1 lists the antibodies used.

Quantitative real-time PCR
The total RNA of heart tissues or cells was isolated by TRIzol® reagent and reverse transcribed using Maxima First Strand cDNA Synthesis Kit, as recommended by the manufacturer. RT-qPCR was performed with real-time PCR detection equipment (Roche, 04896866001), equipped with Light Cycler 480 SYBR Green Master Mix. Supplementary Table S2 lists the primers used.

Statistical analysis
This study used GraphPad Prism 8 to analyze the results, which are presented as mean ± standard error of the mean (SEM). The experiments were designed to generate equal-sized groups by randomization and blinded analyses, with no data points excluded. Blinded analyses were conducted. To evaluate comparisons between multiple groups, Tukey's *post hoc* test was used while Student's *t*-test was used for comparisons between two groups. We considered $P < 0.05$ to be statistically significant.

RESULTS

Macrod1 expression declines in vivo and vitro diabetic cardiomyopathy models
We established a mice DCM model by feeding high-fat diet (HFD) for 16 weeks and intraperitoneally injecting STZ for subsequent experiments. To reveal the potential role of Macrod1 in DCM, we detected the protein levels of MACROD1 in left ventricular myocardial tissue. As shown in Fig. 1a, b, Western blotting results showed a significant increase in brain natriuretic peptide (BNP) in DCM heart tissue and a significant decrease in MACROD1. Correspondingly, in the DCM cell model based on primary cardiomyocytes stimulated by palmitic acid (PA, 400 μM), Western blotting showed that MACROD1 was significantly decreased while BNP was increased after PA was stimulated compared with the control group (Fig. 1c, d). Moreover, immunofluorescence staining showed that Macrod1 and α-actinin were significantly co-localized, suggesting that Macrod1 is mainly expressed in cardiomyocytes (Fig. 1e). To further clarify the main cell types involved in MACROD1 downregulation, we isolated Neonatal Rat Cardiomyocytes (NRCMs), Neonatal Rat Fibroblasts (NRCFs), and Endothelial Cells (ECs) in vitro. As shown in Fig. 1f, *Macrod1* mRNA level was significantly downregulated in NRCMs under PA stimulation, but there was no significant change in NRCFs and ECs cells. These findings indicated that MACORD1 was downregulated mainly in cardiomyocytes. Therefore, to further explore the role of MACROD1 in diabetic cardiomyopathy and the potential mechanism, we constructed Macrod1-KO mice (Supplementary Fig. S1a). Genotyping and DNA sequencing results showed that Macrod1 was successfully knocked out in mice (Supplementary Fig. S1b, c). Meanwhile, Macrod1-KO mouse heart tissue strongly inhibited Macrod1 protein expression in contrast to WT mice (Supplementary Fig. S2a, b).

Macrod1-KO worsens cardiac remodeling and blood glucose regulation in DCM mice
Firstly, we constructed the DCM model as shown in Fig. 2a and assessed the influence of MACROD1 knockout in vivo in different

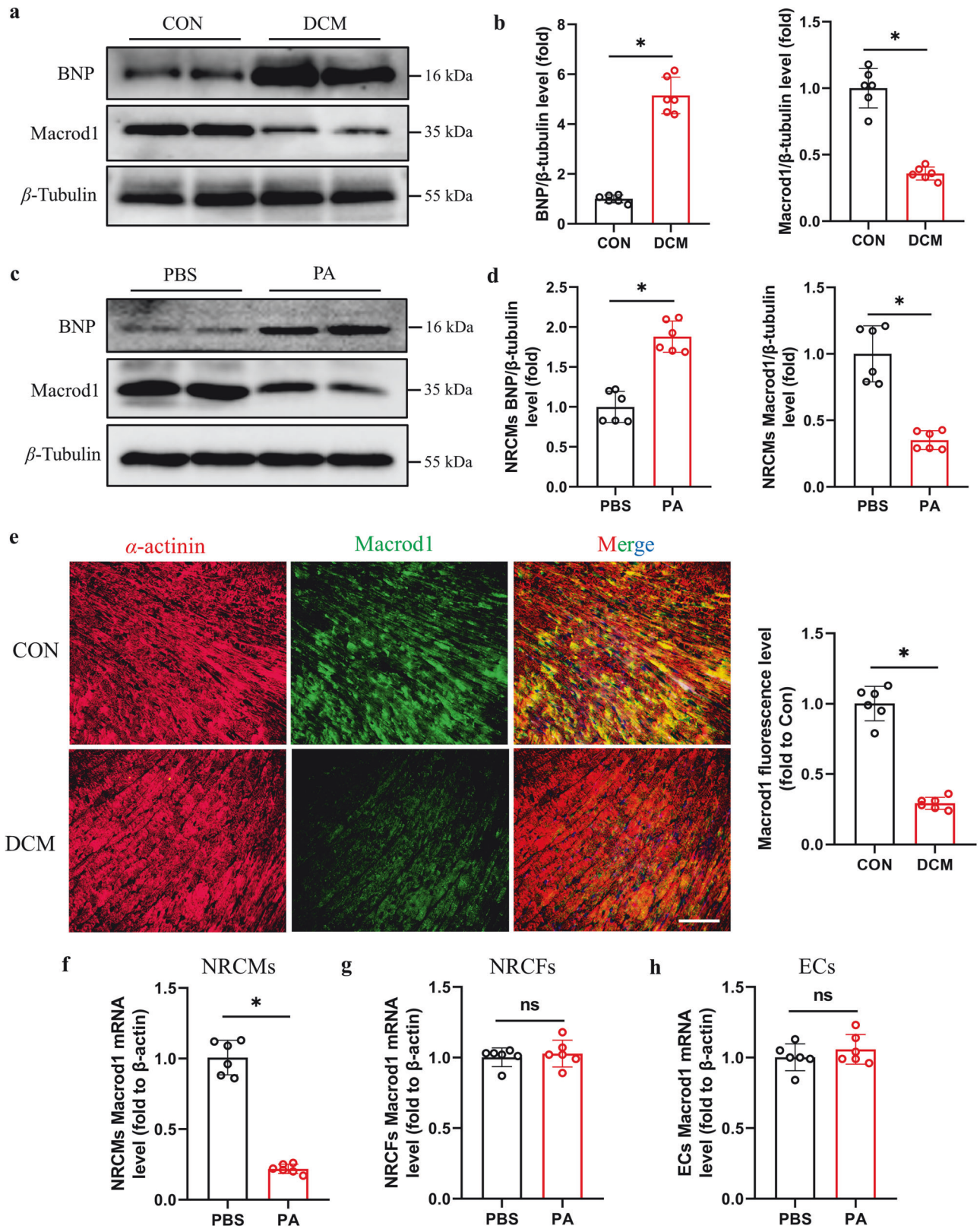

Fig. 1 Macrod1 expression declines in diabetic cardiomyopathy in vivo and in vitro. a Representative Western blotting images and (**b**) quantitative results of BNP and Macrod1 expression in left ventricle tissues from CON or DCM mice ($n = 6$ per group). β-Tubulin served as an internal control. **c** Representative Western blotting images and (**d**) quantitative results of BNP and Macrod1 expression in NRCMs treated with PBS or PA ($n = 6$ per group). β-Tubulin served as an internal control. **e** Representative images and quantification of Macrod1 and α-actinin immunofluorescence staining in heart sections (scale bar = 100 μm, $n = 6$ per group). **f**–**h** Relative mRNA levels of Macrod1 in NRCMs, NRCFs and ECs treated with PBS or PA normalized to β-actin ($n = 6$ per group). Each point represents an independent experiment. All data are presented as the mean ± SEM. One-way analysis of variance (ANOVA) followed by Tukey *post hoc* test was conducted. ns not significant, $^*P < 0.05$.

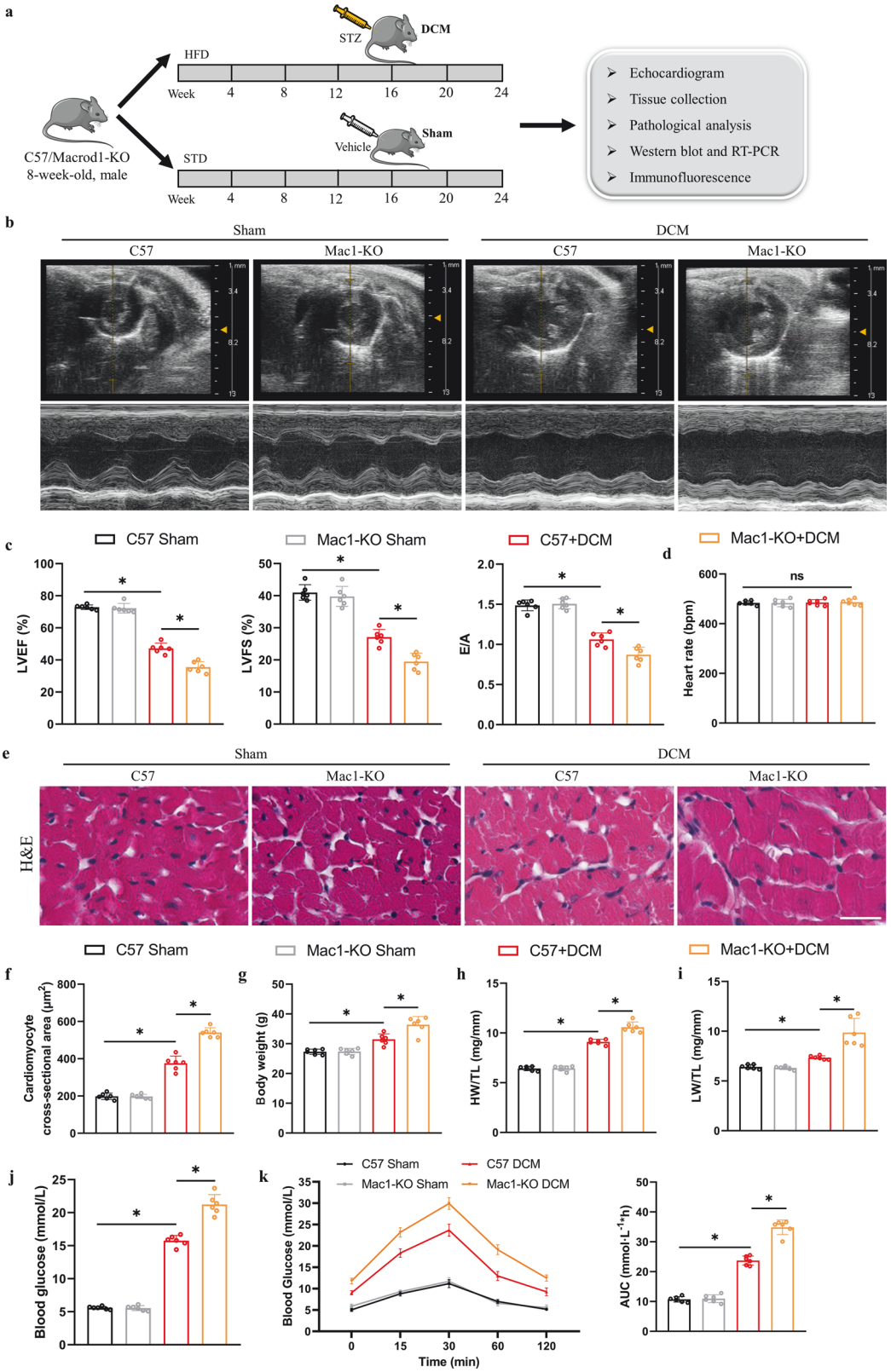

Fig. 2 Macrod1 knockout facilitates cardiac remodeling and dysfunction in DCM. a Experimental timeline for the development of DCM model. **b** Representative images of echocardiography in mice. **c**, **d** Analyses of cardiac function in mice including left ventricular ejection fraction (LVEF), left ventricular fraction shortening (LVFS), E/A ratio and heart rate ($n = 6$ per group). **e**, **f** Representative images of hematoxylin-eosin (H&E) staining in left ventricular sections and quantification of cardiomyocyte cross-sectional area (scale bar= 50 μm, $n = 6$ per group). **g**–**i** Statistical analysis of body weight, HW/TL and LW/TL ratios ($n = 6$ per group). **j** Fasting blood glucose in mice ($n = 6$ per group). **k** Glucose levels in serum samples following a glucose tolerance test in mice ($n = 6$ per group). All data are presented as the mean ± SEM. One-way analysis of variance (ANOVA) followed by Tukey *post hoc* test was conducted. ns not significant, $^*P < 0.05$.

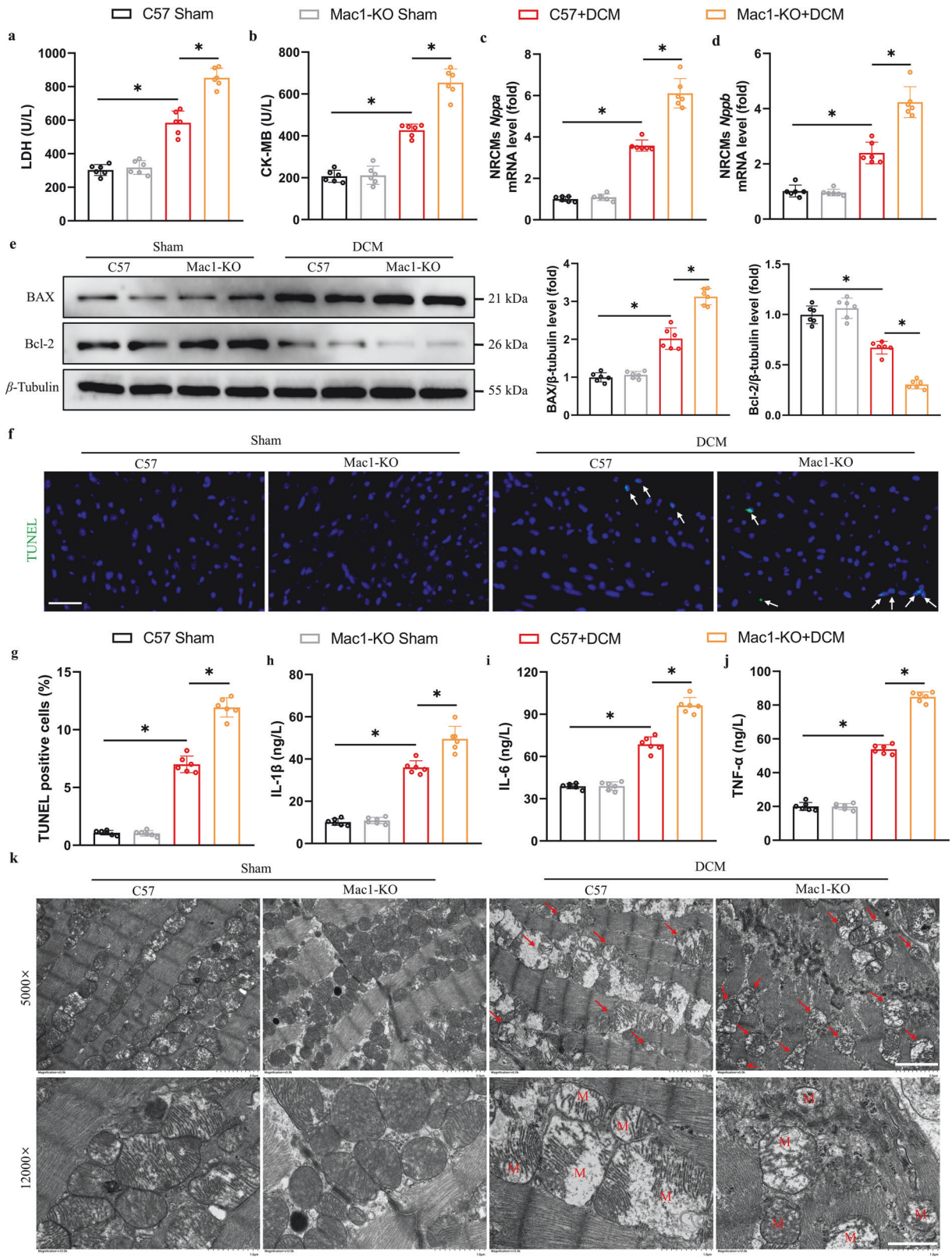

Fig. 3 Macrod1 knockout facilitates cardiac remodeling and dysfunction in DCM. a, **b** Quantification of serum levels of LDH and CK-MB ($n = 6$ per group). **c**, **d** Relative mRNA levels of *Nppa* and *Nppb* in left ventricle tissues, normalized to β-actin ($n = 6$ per group). **e** Representative Western blotting images and quantitative results of BAX and Bcl-2 expression in left ventricle tissues ($n = 6$ per group). β-Tubulin served as an internal control. (**f**, **g**) Representative images and quantitative results of TUNEL staining to detect apoptosis in heart sections ($n = 6$ per group). **h**–**j** The levels of IL-1β, IL-6 and TNF-α in hearts were detected using Elisa kits ($n = 6$ per group). **k** Representative images of Transmission Electron Microscopy (TEM) in heart sections (scale bar = 2 μm for 5000× magnification; scale bar = 1 μm for 12,000× magnification; $n = 6$ per group), red arrows highlight the damaged mitochondria. All data are presented as the mean ± SEM. One-way analysis of variance (ANOVA) followed by Tukey *post hoc* test was conducted. ns not significant, $^*P < 0.05$.

dimensions. The echocardiographic data showed that the DCM group exhibited statistically worse cardiac function. Notably, Macrod1-KO further exacerbated the deterioration of cardiac function in DCM mice. Cardiac function indicators including left ventricular ejection fraction (LVEF), left ventricular fraction shortening (LVFS) and E/A ratio have been dramatically downgraded while there was no significant change in cardiac function in Macrod1-KO mice at the basal physiological level (Fig. 2b, c), and heart rate remained no statistical difference between groups (Fig. 2d). To further evaluate the cardiac contraction and diastolic function of DCM mice, we analyzed the myocardial strain of the left ventricular long axis of the hearts of each group of mice by two-dimensional speckle tracking imaging (Vevo Strain) (Fig. S3A). In Fig. S3B, C, it appears that DCM mice' myocardial global longitudinal strain (GLS%) and long axis radial strain% were significantly deregulated, whereas Macrod1-KO was further downregulated. Accordingly, Macrod1-KO further upregulated the DCM mouse radial strain maximum opposing wall delay% (Supplementary Fig. S3d). In addition, we analyzed the effects of Macrod1-KO on the general heart and myocardial morphology of DCM mice. The results of H&E staining showed that Macrod1-KO aggravated the arrangement disorder of cardiomyocytes and further increased the cross-sectional area of cardiomyocytes in DCM mice (Fig. 2e, f). The results of the modeling endpoint showed that DCM mice had significant increases in body weight (BW), heart weight to tibial length (HW/TL) and lung weight to tibial length (LW/TL) of DCM, while Macrod1-KO further exacerbated these changes (Fig. 2g–i).

Moreover, to better understand the effect of Macrod1-KO on glycemic control in diabetic mice, we measured fasting glucose levels and glucose tolerance tests (OGTTs) in diabetic mice. As Fig. 2j shows, Macrod1-KO mice displayed an increased fasting blood glucose level. Furthermore, Macrod1-KO further impaired glucose tolerance in diabetic mice (Fig. 2k).

Macrod1-KO upregulates inflammation, apoptosis, and aggravates mitochondrial dysfunction in DCM mice

As well as changes in cardiac function and myocardial morphology, DCM has been reported had a closely association with chronic inflammation and apoptosis [26–28]. Therefore, we further examined myocardial injury, inflammation, and apoptosis in mice in each group. Using biochemical analysis to examine the effects of Macrod1-KO on DCM mice, it was shown that Macrod1-KO upregulated myocardial injury markers, such as LDH and CK-MB (Fig. 3a, b). Consistent with this, Macrod1-KO upregulated *Nppa* and *Nppb* mRNA expression levels in heart tissue in DCM mice models (Fig. 3c, d). Meanwhile, according to Western blotting and TUNEL staining results, Macrod1-KO further increased apoptosis levels in DCM mice (Fig. 3e–g). To evaluate how Macrod1-KO affects myocardial inflammation in DCM mice, ELISA was used to test the inflammatory factors levels in plasma. The results of these kits showed that compared with the DCM group, Macrod1-KO further expressed dramatically higher levels of inflammatory factors such as IL-1β, IL-6, and TNF-α (Fig. 3h–j). Furthermore, as previous studies have shown that mitochondrial dysfunction plays a key role in the development of diabetic cardiomyopathy, we assessed mitochondrial morphology in heart tissue by transmission electron microscopy [26, 29]. As shown in Fig. 3k, Macrod1-KO significantly exacerbates mitochondrial damage in cardiomyocytes of DCM mice, and specific manifestations include mitochondrial disorder, swelling, increased vacuoles, fragmented mitochondrial cristae, and reduced mitochondrial cristae density.

Macrod1-KO accelerates oxidative stress injury and disrupts energy metabolism in DCM mice

Multiple previous studies have demonstrated that myocardial energy metabolism dysfunction and oxidative stress in DCM share similar pathophysiological characteristics [30, 31]. According to our results above, Macrod1-KO impaired mitochondrial structure

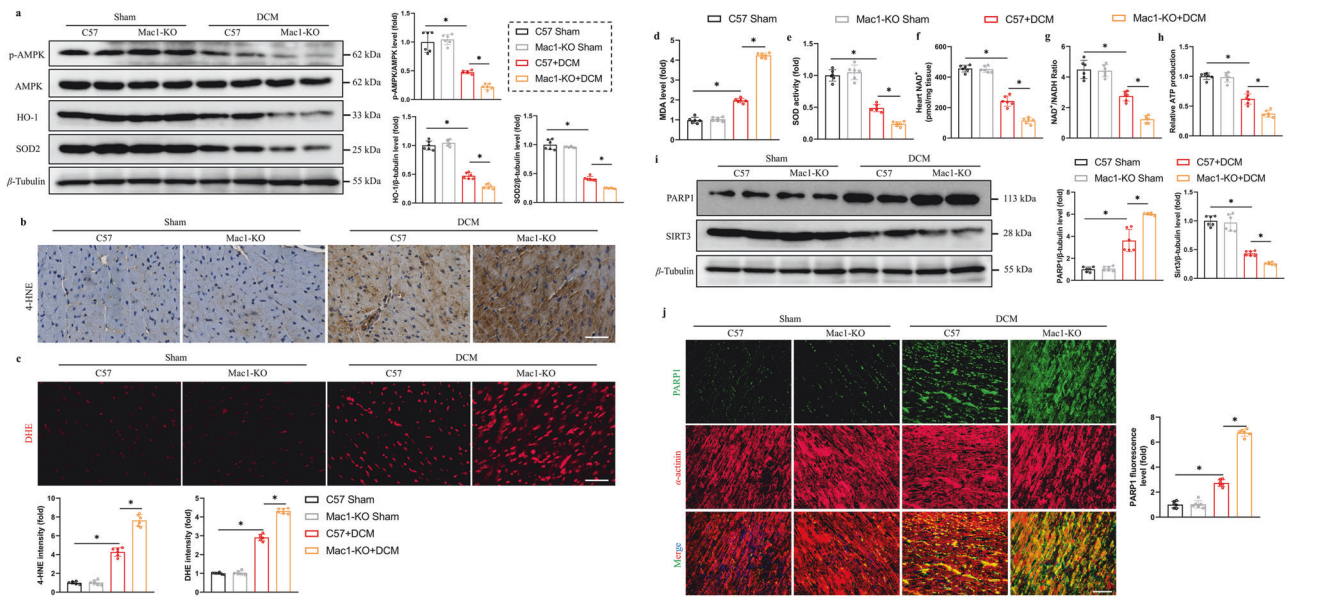

Fig. 4 Macrod1 knockout promotes myocardial oxidative stress and energy deficiency in DCM. a Representative Western blotting images and quantitative results of p-AMPK, AMPK, HO-1 and SOD2 expression in left ventricle tissues ($n = 6$ per group). β-Tubulin served as internal control. **b** Representative images of 4-hydroxyneonal (4-HNE) staining in left ventricular sections and quantification of 4-HNE intensity (scale bar = 100 μm, $n = 6$ per group). **c** Representative images of dihydroethidium (DHE) staining in left ventricular sections and quantification of DHE intensity (scale bar = 100 μm, $n = 6$ per group). **d**, **e** Quantification of MDA levels and total SOD activity in left ventricular tissues ($n = 6$ per group). **f**, **g** Quantification of NAD^+ levels and NAD^+/NADH ratio in left ventricular tissues ($n = 6$ per group). **h** Relative quantification of mitochondrial ATP production levels in mice' hearts ($n = 6$ per group). **i** Representative Western blotting images and quantitative results of PARP1 and SIRT3 expression in left ventricle tissues ($n = 6$ per group). β-Tubulin served as an internal control. **j** Representative images and quantification of PARP1 and α-actinin immunofluorescence staining in heart sections (scale bar = 100 μm, $n = 6$ per group). All data are presented as the mean ± SEM. One-way analysis of variance (ANOVA) followed by Tukey *post hoc* test was conducted. ns not significant, $^*P < 0.05$.

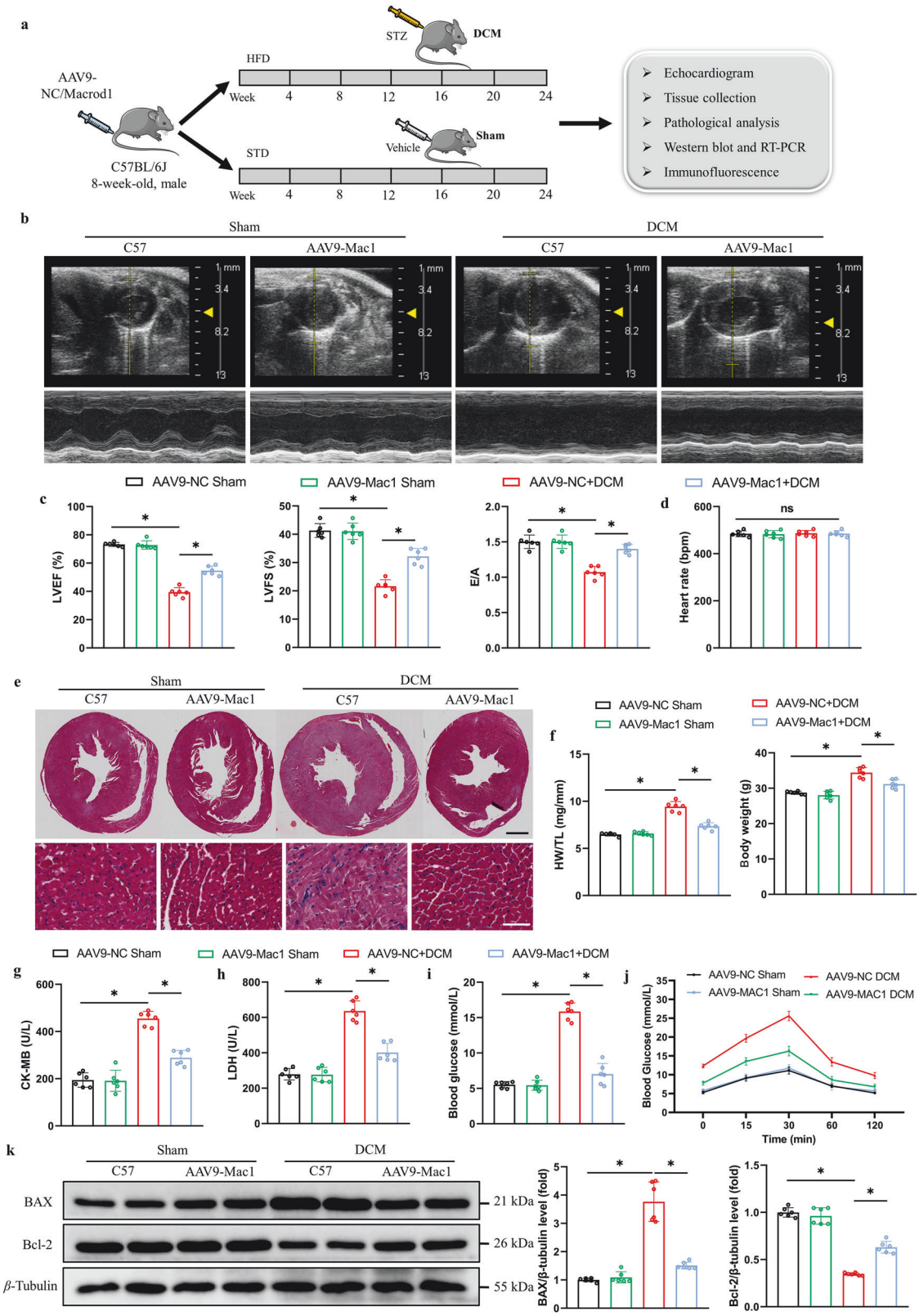

in DCM mice. In this regard, we hypothesize that Macrod1 may affect diabetic cardiomyopathy progression by modulating oxidative stress damage and disrupting energy metabolism. As expected, Western blotting results showed that Macrod1-KO further downregulated the protein levels of p-AMPK, HO-1 and SOD2 (Fig. 4a). Furthermore, 4-HNE and DHE staining results also indicated that Macrod1-KO upregulated oxidative stress levels of the heart in vivo DCM models (Fig. 4b, c). Correspondingly, Macrod1-KO stimulated MDA levels and diminished total SOD activity in DCM myocardial tissue (Fig. 4d, e). Based on these

Fig. 5 Cardiac-specific Macrod1 overexpression alleviates cardiac remodeling and dysfunction in DCM. a Experimental timeline for the development of Cardiac-specific Macrod1 overexpression and DCM model. **b** Representative images of echocardiography in left ventricle. **c**, **d** Analyses of cardiac function in mice including LVEF, LVFS, E/A ratio and heart rate ($n = 6$ per group). **e** Representative images of H&E staining in left ventricular sections (scale bar = 1 mm for 10× magnification; scale bar = 50 μm for 400× magnification, $n = 6$ per group). **f** Statistical analysis of body weight and HW/TL ratios ($n = 6$ per group). **g**, **h** Quantification of serum levels of CK-MB and LDH ($n = 6$ per group). **i** Fasting blood glucose in each group mice ($n = 6$ per group). **j** Glucose levels in serum samples following a glucose tolerance test ($n = 6$ per group). **k** Representative Western blotting images and quantitative results of BAX and Bcl-2 expression in left ventricle tissues ($n = 6$ per group). β-Tubulin served as an internal control. All data are presented as the mean ± SEM. One-way analysis of variance (ANOVA) followed by Tukey *post hoc* test was conducted. ns not significant, $^*P < 0.05$.

findings, it appears that Macrod1 knockout can worsen myocardial oxidative stress and damage the antioxidant system in DCM.

Recent studies have demonstrated that NAD^+ plays a crucial role in oxidative stress repair and mitochondrial function [32]. Hence, we examined NAD^+ levels in cardiac tissue. As shown in Fig. 4f, g, NAD^+ levels are downregulated in diabetic hearts, and Macrod1-KO further significantly downregulated NAD^+ levels. To further explore mitochondria's energetic status, we examined mice' cardiomyocyte ATP production in each group. As shown in Fig. 4h, Macrod1-KO further exacerbates ATP production down-regulation, indicating that Macrod1 deletion impairs energy metabolism in DCM mice. As PARP1 has been reported to exert its biological activity in a very consuming NAD^+ way [33], while SIRT3 is a NAD^+-dependent deacetylase and the two are both important to mitochondrial, we detected the protein levels of PARP1 and SIRT3. As shown in Fig. 4i, j, Macrod1-KO enhanced PARP1 expression while decreasing SIRT3 expression in DCM myocardial tissue, which may be the primary reason for the massive consumption of NAD^+ in the heart. Alternatively, previous studies revealed that CK mito and thioredoxin 2 (Trx2) play critical roles in heart failure and antioxidant stress [5, 34, 35]. As shown in Supplementary Fig. S4a, b, CK mito and Trx2 are significantly downregulated in DCM hearts, whereas Macrod1-KO hearts do not show significant changes.

Macrod1 overexpression improves diabetic myocardial disorder in mice

To determine whether Macrod1 overexpression can improve myocardial injury in diabetic cardiomyopathy, we constructed a vector with an AAV9-*Macrod1* overexpression specific for cardiomyocytes. Referring to Fig. 5a, the mice' tail vein was injected with the AAV9-NC or AAV9-*Macrod1* virus. We randomly divided the mice into a control group and a DCM group after stable overexpression in the heart. Moreover, Western blotting and immunofluorescence staining results indicated that AAV9-*Macrod1* was significantly overexpressed in cardiomyocytes (Supplementary Fig. S5a, b). Next, we assessed cardiac function and cardiac pathological morphology in each group of mice. As shown in Fig. 5b, c, echocardiography reveals that Macrod1 overexpression in cardiomyocytes can significantly alleviate cardiac systolic and diastolic dysfunction in DCM, and heart rate remained no significant difference between groups (Fig. 5d). Consistent with this, the results of H&E staining, HW/TL, body weight, CK-MB, and LDH confirmed that Macrod1 overexpression effectively improved myocardial remodeling and myocardial injury in DCM (Fig. 5e–h). More importantly, Macrod1 overexpression improved fasting blood glucose and glucose tolerance in DCM mice (Fig. 5i, j). Furthermore, Macrod1 overexpression decreased cardiomyocyte apoptosis in DCM mice (Fig. 5k). Additionally, Macrod1 overexpression reduced cardiac inflammation levels in mice (Supplementary Fig. S6a–c).

As Macrod1-KO aggravated cardiac oxidative stress in DCM mice, we examined whether Macrod1 overexpression could improve cardiac oxidative stress levels in the disease. As shown in Fig. 6a, Macrod1 overexpression significantly alleviated the downregulation of HO-1 and SOD2 levels in myocardial tissue of DCM mice. Meanwhile, 4-HNE and DHE staining results of mouse heart-frozen sections suggested that overexpression of Macrod1 decreased lipid peroxidation and reactive oxygen species in myocardial tissue (Fig. 6b, c). Besides, Macrod1 overexpression improved MDA and total SOD activity levels (Fig. 6d, e). Most notably, Macrod1 overexpression greatly increased cardiac NAD^+ levels in DCM (Fig. 6f, g). Mechanically, Macrod1 overexpression reverses PARP1 upregulation and alleviates SIRT3 protein downregulation in DCM mice' hearts (Fig. 6h). Accordingly, Macrod1 appears to mitigate oxidative stress through PARP1-NAD^+-SIRT3 signaling.

Overexpressed Macrod1 in cardiomyocytes ameliorates PA-induced oxidative stress injury

To further elucidate the mechanism of Macrod1 in diabetic cardiomyopathy, we established an in vitro cardiomyocyte model of Macrod1 overexpression by infecting NRCMs with Ad-*Macrod1*. According to the determination of MDA levels and total SOD activity in cardiomyocytes, we found that Macrod1 overexpression alleviated PA-induced oxidative stress in cardiomyocytes (Fig. 7a, b). Similar to the in vivo DCM model, PA stimulation significantly reduced NAD^+ levels in cardiomyocytes, which was partially alleviated by Macrod1 overexpression (Fig. 7c, d). Mechanically, PA down-regulated HO-1, SOD2, and SIRT3, while up-regulating PARP1 protein levels in NRCMs, which could be partially compensated by overexpressing Macrod1 (Fig. 7e). As shown by DCFH-DA staining of cardiomyocytes, Macrod1 overexpression inhibits PA-induced ROS production (Fig. 7f). Additionally, JC-1 staining was used to investigate mitochondrial damage in NRCMs, a major driver of cardiomyocyte damage in diabetes. As shown in Fig. 7g, Macrod1 overexpression significantly improved PA-induced mitochondrial membrane potential abnormalities in cardiomyocytes.

Macrod1 improves oxidative stress by regulating the PARP1-NAD^+-SIRT3 pathway

Recent study has demonstrated that PARP1 interacts with SIRT3 to regulate isoproterenol-induced cardiac hypertrophy [36], while our results indicate that Macrod1 can partly reverse PARP1 upregulation and SIRT3 downregulation in DCM (Figs. 5–7). As a result, we hypothesize that Macrod1 involved in oxidative stress in diabetic cardiomyopathy by regulating the PARP1-NAD^+-SIRT3 signaling pathway. Aiming to gain insight into Macrod1 regulation mechanisms, we intervened in the key genes and molecules of the PARP1-NAD^+-SIRT3 signaling pathway in a cardiomyocyte model.

Macrod1 knockdown further elevated PA-induced MDA levels and depressed PA-induced total SOD activity, but NA supplementation partially reversed these effects (Fig. 8a, b). Western blotting results revealed that Macrod1-KO further decreased the PA-induced SIRT3-SOD2/HO-1 pathway activation level, and increased PARP1 protein level, which can be inhibited by NA (Fig. 8c). In addition to this, DCFH-DA and JC-1 staining suggested that Macrod1-KO caused a further increase in ROS concentrations and damage to mitochondrial membrane potential, both of which were ameliorated by NA (Fig. 8d–f). In view of the critical role of SIRT3 in DCM oxidative stress, we applied si-RNA to knock down SIRT3 expression in cardiomyocytes to further explore the mechanism of Macrod1. As shown in Fig. 8g, inhibiting SIRT3

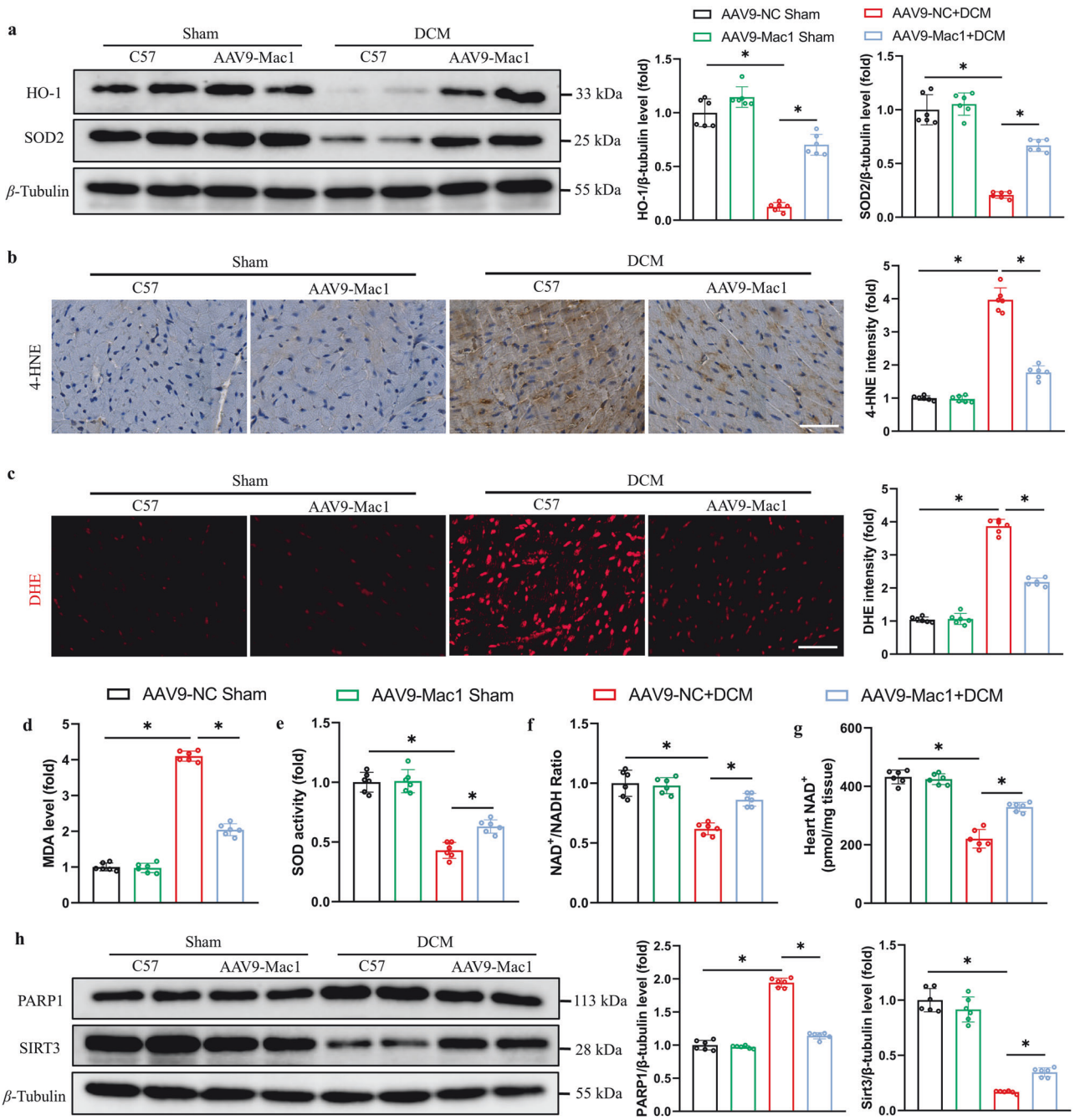

Fig. 6 Cardiac-specific Macrod1 overexpression ameliorates oxidative stress in DCM. a Representative Western blotting images and quantitative results of HO-1 and SOD2 expression in left ventricle tissues ($n = 6$ per group). β-Tubulin served as an internal control. **b** Representative images of 4-HNE staining in left ventricular sections and quantification of 4-HNE intensity (scale bar = 100 μm, $n = 6$ per group). **c** Representative images of DHE staining in left ventricular sections and quantification of DHE intensity (scale bar = 100 μm, $n = 6$ per group). **d**, **e** Quantification of MDA levels and total SOD activity in left ventricular tissues ($n = 6$ per group). **f**, **g** Quantification of NAD^+/NADH ratio and NAD^+ levels in left ventricular tissues ($n = 6$ per group). **h** Representative Western blotting images and quantitative results of PARP1 and SIRT3 expression in left ventricular tissues ($n = 6$ per group). β-Tubulin served as an internal control. All data are presented as the mean ± SEM. One-way analysis of variance (ANOVA) followed by Tukey *post hoc* test was conducted. ns not significant, $^*P < 0.05$.

expression abolishes the protective effect of Macrod1 overexpression on PA-induced cardiomyocytes. Accordingly, the overexpression of Macrod1 increases HO-1 and SOD2 protein levels, but SIRT3 knockdown suppresses these changes. DCFH-DA and JC-1 staining further confirmed that SIRT3 knockdown weakened Macrod1 overexpression's protective effect on PA-induced oxidative stress in cardiomyocytes. As shown in Fig. 8h, overexpressing Macrod1 suppressed the PA-induced increase in ROS levels and decrease in mitochondrial membrane potential, whereas SIRT3 knockdown blocked this protective effect. Moreover, SIRT3 knockout further increased myocardial apoptosis and eliminated Macrod1 overexpression's ameliorative effect on cardiomyocyte apoptosis (Supplementary Fig. S7a, b). In light of this, Macrod1 might serve as a therapeutic target in diabetic cardiomyopathy. It could also provide an alternative therapeutic direction for diabetic cardiomyopathy clinical treatment.

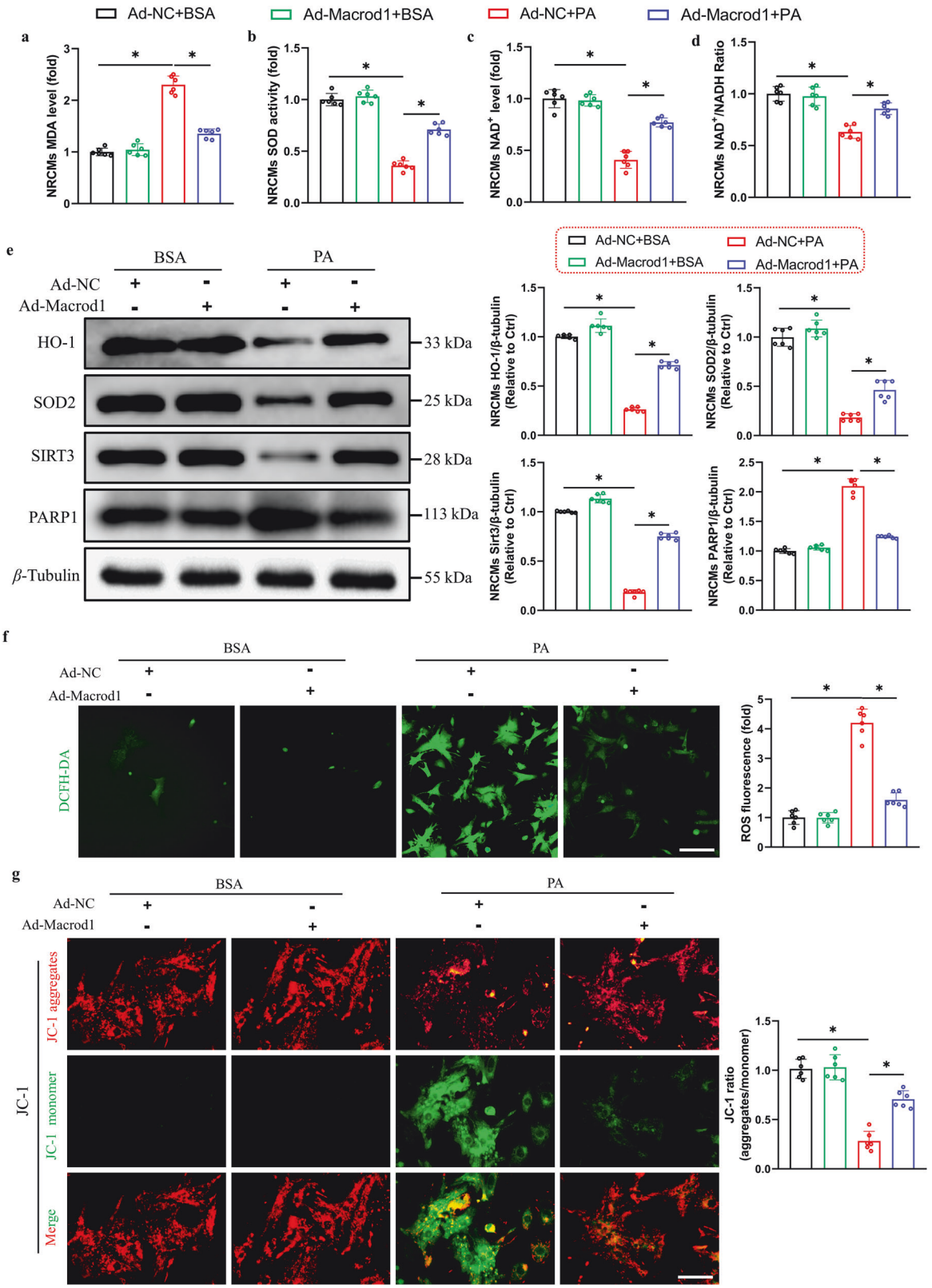

Fig. 7 Cardiomyocyte Macrod1 overexpression alleviates PA-induced oxidative stress damage. a, **b** Quantification of MDA levels, total SOD activity in NRCMs ($n = 6$ per group). **c**, **d** Quantification of NAD^+ levels and NAD^+/NADH ratio in NRCMs ($n = 6$ per group). **e** Representative Western blotting images and quantitative results of HO-1, SOD2, Sirt3 and PARP1 expression in NRCMs ($n = 6$ per group). β-Tubulin served as an internal control. **f** Representative images of DCFH-DA staining in NRCMs and quantification of ROS fluorescence (scale bar = 100 μm, $n = 6$ per group). **g** Representative images of JC-1 staining in NRCMs and quantification of JC-1 aggregates/monomer fluorescence (scale bar = 50 μm, $n = 6$ per group). All data are presented as the mean ± SEM. One-way analysis of variance (ANOVA) followed by Tukey *post hoc* test was conducted. ns not significant, $^*P < 0.05$.

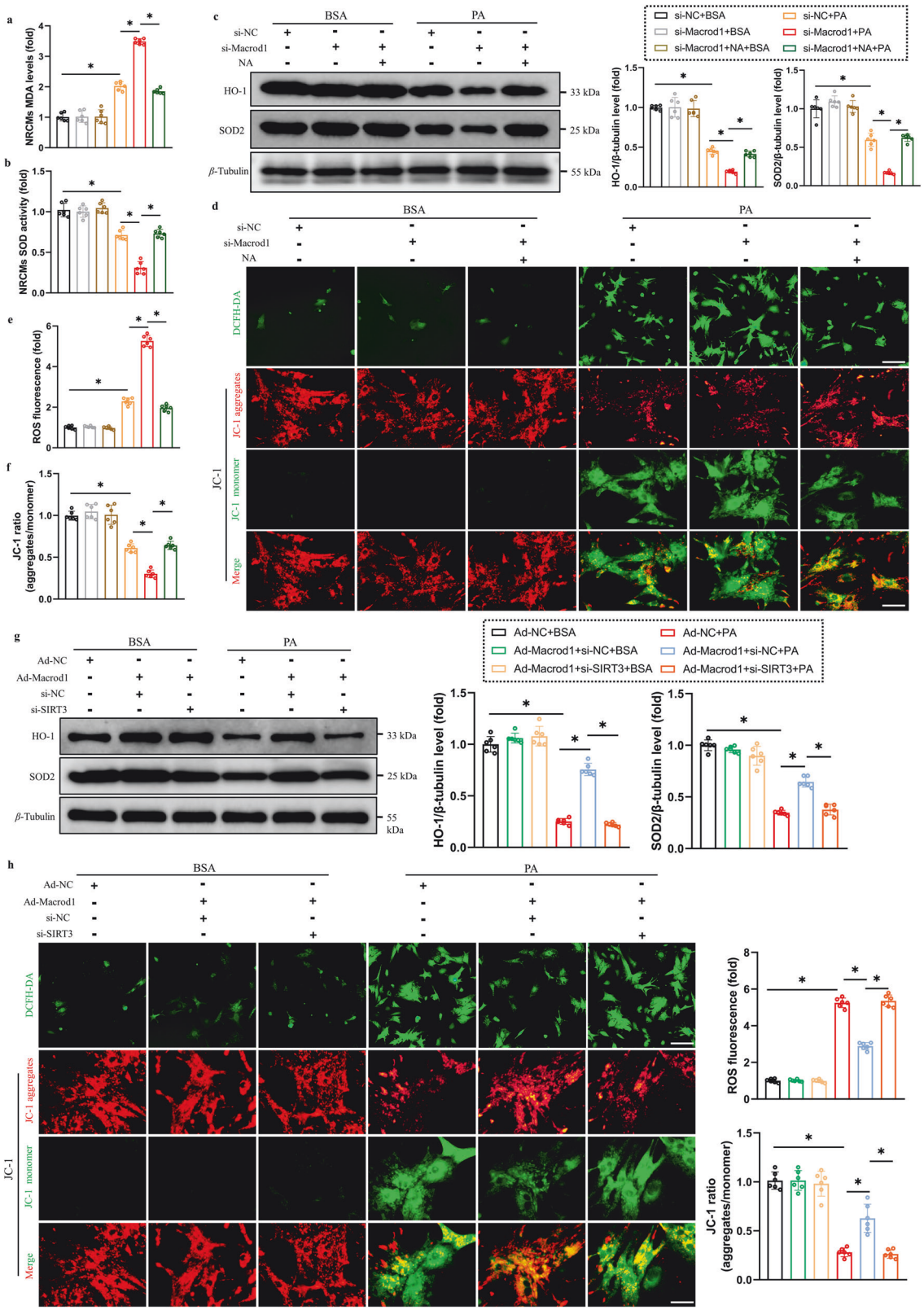

DISCUSSION

In the present study, we revealed for the first time the role of Macrod1 in diabetic heart and its underlying mechanism. Specifically, this study innovatively demonstrates: (a) Macrod1 expression is significantly downregulated in diabetic cardiomyopathy in vivo and in vitro, which is associated with worsening cardiac function; (b) Macrod1 knockout exacerbates cardiac remodeling, mitochondrial dysfunction, and oxidative stress in

Fig. 8 Macrod1 improves oxidative stress by regulating the PARP1-NAD$^+$-SIRT3 pathway. a, **b** Quantification of MDA levels, total SOD activity in NRCMs ($n = 6$ per group). **c** Representative Western blotting images and quantitative results of HO-1, SOD2, Sirt3 and PARP1 expression in NRCMs ($n = 6$ per group). β-Tubulin served as internal control. **d–f** Representative images of DCFH-DA and JC-1 staining in NRCMs, and quantification of ROS fluorescence and JC-1 aggregates/monomer fluorescence (DCFH-DA staining scale bar = 100 μm, JC-1 staining scale bar = 50 μm, $n = 6$ per group). **g** Representative Western blotting images and quantitative results of HO-1 and SOD2 expression in NRCMs ($n = 6$ per group). β-Tubulin served as internal control. **h** Representative images of DCFH-DA and JC-1 staining in NRCMs, and quantification of ROS fluorescence and JC-1 aggregates/monomer fluorescence (DCFH-DA staining scale bar = 100 μm, JC-1 staining scale bar = 50 μm, $n = 6$ per group). All data are presented as the mean ± SEM. One-way analysis of variance (ANOVA) followed by Tukey *post hoc* test was conducted. ns not significant, $^*P < 0.05$.

DCM, and Macrod1 overexpression can partly reverse these pathological processes in the DCM models; (c) Mechanistically, Macrod1 inhibits PARP1 expression and restores NAD$^+$ levels, thereby activating SIRT3 to resist oxidative stress. More importantly, NAD$^+$ precursor NA supplementation alleviates oxidative stress in PA-stimulated cardiomyocytes. Therefore, targeting the restoration of Macrod1 and NAD$^+$ levels in cardiomyocytes may provide a potential clinical therapeutic target for DCM treatment.

Diabetes mellitus disease burden is gradually increasing, with a global prevalence of 10.5% in 2021 (affecting 537 million people), and this number is expected to rise to 12.2% (affecting 783 million people) by 2045 [37]. And crucially, DCM is the leading cause of mortality in T2DM patients [37, 38]. Diabetic cardiomyopathy is a progressive process, developing from early diastolic dysfunction to heart failure, accompanied by a variety of pathophysiological mechanisms. The mechanism of DCM is complex, involving mitochondrial structure and dysfunction, NAD$^+$ reduction, oxidative stress, inflammation and apoptosis [39, 40]. In this study, we constructed a DCM model by feeding a high-fat diet (HFD) for 16 weeks and intraperitoneally injecting STZ. Deterioration of cardiac function, increased apoptosis, mitochondrial damage and ROS accumulation were observed in DCM mice. The above pathological changes were further worsened by Macrod1 knockout, but alleviated by Macrod1 overexpression and NA supplementation. Previous studies have shown that activating SIRT3 and improving downstream oxidative stress levels can reduce blood glucose levels and improve insulin resistance in DCM mice [41, 42]. Consistent with this, we found that Macrod1 knockout aggravated impaired blood glucose levels and glucose tolerance in DCM mice by inhibiting SIRT3 and its downstream anti-oxidative stress pathways. On the contrary, overexpression of Macrod1 can improve systemic blood glucose metabolism and glucose tolerance in diabetic mice, suggesting that Macrod1 may improve diabetes multi-systemically. And Macrod1's potential role in blood glucose regulation and other organs requires further study in the future.

Macrod1 is a mono-ADP-ribosylating hydrolase, but its physiological function and role in disease remain largely unknown. Previous studies have suggested that Macrod1 is mainly localized in mitochondria, and Macrod1 knockout will lead to motor-coordination defects [8, 43]. However, the role and underlying mechanism of Macrod1 in DCM have not been reported. In this study, we found for the first time that Macrod1 is significantly downregulated in cardiomyocytes in DCM. ROS and JC-1 staining results showed that Macrod1 knockout further exacerbates mitochondrial damage and oxidative stress in diabetic cardiomyopathy, while Macrod1 overexpression partially alleviates it. Mechanistically, Macrod1 knockout further upregulated PARP1 expression, massively depleting NAD$^+$ levels in DCM. PARP1 is one of the main NAD$^+$ consuming enzymes and can participate in a variety of biological processes by consuming ATP and NAD$^+$ [44, 45]. Furthermore, we found that supplementing NA, the precursor of NAD$^+$, can effectively alleviate oxidative stress and cardiomyocyte damage caused by Macrod1 knockdown and PA stimulation in vitro NRCMs. Recent studies have shown that PARP1 affects blood-brain barrier damage by regulating NAD$^+$ levels, leading to abnormal mitophagy and SIRT3 degradation [44]. This suggests that SIRT3, as an NAD$^+$-dependent deacetylase, has a potential connection with PARP1. Therefore, to further explore Macrod1's molecular mechanism, we detected SIRT3 expression in vivo and in vitro. Results showed that Macrod1 knockdown further reduced SIRT3 levels, while Macrod overexpression significantly restored SIRT3 expression in DCM hearts. In contrast, SIRT3 inhibition abolished the protective effect of Macrod1 overexpression on PA-induced oxidative stress injury in cardiomyocytes. The above results illustrate the innovative role of Macrod1 and create a potential therapeutic target in DCM.

There are some limitations to this study. The specific mechanism and site by which Macrod1 regulates PARP1 remain unclear. We hypothesize that Macrod1 may regulate DCM outcomes by affecting the ADP-ribosylation function of PARP1. Despite the numerous limitations, these will be clarified in the future research.

CONCLUSION

In summary, our work reveals an innovative role for Macrod1 in DCM. Macrod1 knockout exacerbates cardiac dysfunction, mitochondrial damage, and oxidative stress in DCM, which are alleviated by Macrod1 overexpression. Mechanistically, Macrod1 reduces NAD$^+$ consumption by inhibiting PARP1 expression, thereby upregulating the expression and function of SIRT3. These data identify that Macrod1 is a novel target for DCM treatment and that targeting the PARP1-NAD$^+$-SIRT3 axis may develop new intervention strategies in DCM.

ACKNOWLEDGEMENTS

This work was supported by the Regional Innovation and Development Joint Fund of National Natural Science Foundation of China (No. U22A20269) and the National Key R&D Program of China (2018YFC1311300).

AUTHOR CONTRIBUTIONS

QZT, YC, YTL, and HLQ contributed to the design and conception of the study. QZT was responsible for the financial support. YTL and HLQ designed and implemented the majority of the experiments, analyzed the majority of the data and prepared graphs and tables. YTL, HLQ, and YC wrote and edited the manuscript. HXX, YZF, JYD, YY, DK and HZ assisted with some experiments and discussed the results. All authors approved the final version.

ADDITIONAL INFORMATION

Supplementary information The online version contains supplementary material available at https://doi.org/10.1038/s41401-024-01247-2.

Competing interests: The authors declare no competing interests.

REFERENCES

1. Jia G, Whaley-Connell A, Sowers JR. Diabetic cardiomyopathy: a hyperglycaemia- and insulin-resistance-induced heart disease. Diabetologia. 2018;61:21–8.
2. Dillmann WH. Diabetic cardiomyopathy. Circ Res. 2019;124:1160–2.
3. Tan Y, Zhang Z, Zheng C, Wintergerst KA, Keller BB, Cai L. Mechanisms of diabetic cardiomyopathy and potential therapeutic strategies: preclinical and clinical evidence. Nat Rev Cardiol. 2020;17:585–607.

4. Aon MA, Tocchetti CG, Bhatt N, Paolocci N, Cortassa S. Protective mechanisms of mitochondria and heart function in diabetes. Antioxid Redox Signal. 2015;22:1563–86.
5. Keceli G, Gupta A, Sourdon J, Gabr R, Schar M, Dey S, et al. Mitochondrial creatine kinase attenuates pathologic remodeling in heart failure. Circ Res. 2022;130:741–59.
6. Rosenthal F, Feijs KL, Frugier E, Bonalli M, Forst AH, Imhof R, et al. Macrodomain-containing proteins are new mono-ADP-ribosylhydrolases. Nat Struct Mol Biol. 2013;20:502–7.
7. Jankevicius G, Hassler M, Golia B, Rybin V, Zacharias M, Timinszky G, et al. A family of macrodomain proteins reverses cellular mono-ADP-ribosylation. Nat Struct Mol Biol. 2013;20:508–14.
8. Agnew T, Munnur D, Crawford K, Palazzo L, Mikoc A, Ahel I. Macrod1 is a promiscuous ADP-ribosyl hydrolase localized to mitochondria. Front Microbiol. 2018;9:20.
9. O'Connell KS, Koch E, Lenk HC, Akkouh IA, Hindley G, Jaholkowski P, et al. Polygenic overlap with body-mass index improves prediction of treatment-resistant schizophrenia. Psychiatry Res. 2023;325:115217.
10. Zaja R, Aydin G, Lippok BE, Feederle R, Luscher B, Feijs KLH. Comparative analysis of MACROD1, MACROD2 and TARG1 expression, localisation and interactome. Sci Rep. 2020;10:8286.
11. Wu Z, Wang C, Bai M, Li X, Mei Q, Li X, et al. An LRP16-containing preassembly complex contributes to NF-kappaB activation induced by DNA double-strand breaks. Nucleic Acids Res. 2015;43:3167–79.
12. Ordog K, Horvath O, Eros K, Bruszt K, Toth S, Kovacs D, et al. Mitochondrial protective effects of PARP-inhibition in hypertension-induced myocardial remodeling and in stressed cardiomyocytes. Life Sci. 2021;268:118936.
13. Park ES, Kang DH, Kang JC, Jang YC, Lee MJ, Chung HJ, et al. Cardioprotective effect of KR-33889, a novel PARP inhibitor, against oxidative stress-induced apoptosis in H9c2 cells and isolated rat hearts. Arch Pharmacol Res. 2017;40:640–54.
14. Deng Z, He M, Hu H, Zhang W, Zhang Y, Ge Y, et al. Melatonin attenuates sepsis-induced acute kidney injury by promoting mitophagy through SIRT3-mediated TFAM deacetylation. Autophagy. 2024;20:151–65.
15. Zhang J, He Z, Fedorova J, Logan C, Bates L, Davitt K, et al. Alterations in mitochondrial dynamics with age-related Sirtuin1/Sirtuin3 deficiency impair cardiomyocyte contractility. Aging Cell. 2021;20:e13419.
16. Benigni A, Cassis P, Conti S, Perico L, Corna D, Cerullo D, et al. Sirt3 deficiency shortens life span and impairs cardiac mitochondrial function rescued by opa1 gene transfer. Antioxid Redox Signal. 2019;31:1255–71.
17. Gao J, Huang C, Kong L, Zhou W, Sun M, Wei T, et al. SIRT3 regulates clearance of apoptotic cardiomyocytes by deacetylating frataxin. Circ Res. 2023;133:631–47.
18. Hu T, Wu Q, Yao Q, Yu J, Jiang K, Wan Y, et al. PRDM16 exerts critical role in myocardial metabolism and energetics in type 2 diabetes induced cardiomyopathy. Metabolism. 2023;146:155658.
19. Xie S, Zhang M, Shi W, Xing Y, Huang Y, Fang WX, et al. Long-term activation of glucagon-like peptide-1 receptor by dulaglutide prevents diabetic heart failure and metabolic remodeling in type 2 diabetes. J Am Heart Assoc. 2022;11:e026728.
20. Li C, Guo Z, Liu F, An P, Wang M, Yang D, et al. PCSK6 attenuates cardiac dysfunction in doxorubicin-induced cardiotoxicity by regulating autophagy. Free Radic Biol Med 2023;203:114–28.
21. Liu LB, Huang SH, Qiu HL, Cen XF, Guo YY, Li D, et al. Limonin stabilises sirtuin 6 (SIRT6) by activating ubiquitin specific peptidase 10 (USP10) in cardiac hypertrophy. Br J Pharmacol. 2022;179:4516–33.
22. Zhang X, Hu C, Ma ZG, Hu M, Yuan XP, Yuan YP, et al. Tisp40 prevents cardiac ischemia/reperfusion injury through the hexosamine biosynthetic pathway in male mice. Nat Commun. 2023;14:3383.
23. Yang D, Fan D, Guo Z, Liu FY, Wang MY, An P, et al. SENP1 protects against pressure overload-induced cardiac remodeling and dysfunction via inhibiting STAT3 signaling. J Am Heart Assoc. 2022;11:e027004.
24. Xie S, Xing Y, Shi W, Zhang M, Chen M, Fang W, et al. Cardiac fibroblast heat shock protein 47 aggravates cardiac fibrosis post myocardial ischemia-reperfusion injury by encouraging ubiquitin specific peptidase 10 dependent Smad4 deubiquitination. Acta Pharm Sin B 2022;12:4138–53.
25. Che Y, Wang Z, Yuan Y, Zhou H, Wu H, Wang S, et al. By restoring autophagic flux and improving mitochondrial function, corosolic acid protects against Dox-induced cardiotoxicity. Cell Biol Toxicol. 2022;38:451–67.
26. Shi X, Liu C, Chen J, Zhou S, Li Y, Zhao X, et al. Endothelial MICU1 alleviates diabetic cardiomyopathy by attenuating nitrative stress-mediated cardiac microvascular injury. Cardiovasc Diabetol. 2023;22:216.
27. Mohsin S, Wang H, Khan M. Inflammation attenuating lncRNAs in diabetic cardiomyopathy. Mol Ther Nucleic Acids. 2023;34:102029.
28. Zhang L, Luo Y, Lv L, Chen S, Liu G, Zhao T. TRAP1 inhibits MARCH5-mediated MIC60 degradation to alleviate mitochondrial dysfunction and apoptosis of cardiomyocytes under diabetic conditions. Cell Death Differ. 2023;30:2336–50.
29. Zhang N, Yu H, Liu T, Zhou Z, Feng B, Wang Y, et al. Bmal1 downregulation leads to diabetic cardiomyopathy by promoting Bcl2/IP3R-mediated mitochondrial Ca^{2+} overload. Redox Biol. 2023;64:102788.
30. Wang D, Li J, Luo G, Zhou J, Wang N, Wang S, et al. Nox4 as a novel therapeutic target for diabetic vascular complications. Redox Biol. 2023;64:102781.
31. Gopal K, Karwi QG, Tabatabaei Dakhili SA, Wagg CS, Zhang L, Sun Q, et al. Aldose reductase inhibition alleviates diabetic cardiomyopathy and is associated with a decrease in myocardial fatty acid oxidation. Cardiovasc Diabetol. 2023;22:73.
32. Covarrubias AJ, Perrone R, Grozio A, Verdin E. NAD^+ metabolism and its roles in cellular processes during ageing. Nat Rev Mol Cell Biol. 2021;22:119–41.
33. Darshan HR, Sudhir BJ, Singh A, Sreenath R, Easwer HV, Krishnakumar K, et al. Analysis of evolution of hydrocephalus in Posterior Fossa Tumors and validation study of the modified Canadian preoperative prediction rule for hydrocephalus in children and Frankfurt Grading System for prediction of cerebrospinal fluid diversion in adults with Posterior Fossa Tumors. World Neurosurg. 2023;180:e91–8.
34. Tocchetti CG, Caceres V, Stanley BA, Xie C, Shi S, Watson WH, et al. GSH or palmitate preserves mitochondrial energetic/redox balance, preventing mechanical dysfunction in metabolically challenged myocytes/hearts from type 2 diabetic mice. Diabetes. 2012;61:3094–105.
35. Stanley BA, Sivakumaran V, Shi S, McDonald I, Lloyd D, Watson WH, et al. Thioredoxin reductase-2 is essential for keeping low levels of H_2O_2 emission from isolated heart mitochondria. J Biol Chem. 2011;286:33669–77.
36. Feng X, Wang Y, Chen W, Xu S, Li L, Geng Y, et al. SIRT3 inhibits cardiac hypertrophy by regulating PARP-1 activity. Aging (Albany NY). 2020;12:4178–92.
37. Marx N, Federici M, Schutt K, Muller-Wieland D, Ajjan RA, Antunes MJ, et al. 2023 ESC Guidelines for the management of cardiovascular disease in patients with diabetes. Eur Heart J. 2023;44:4043–140.
38. Lezoualc'h F, Badimon L, Baker H, Bernard M, Czibik G, de Boer RA, et al. Diabetic cardiomyopathy: the need for adjusting experimental models to meet clinical reality. Cardiovasc Res. 2023;119:1130–45.
39. Guo Z, Tuo H, Tang N, Liu FY, Ma SQ, An P, et al. Neuraminidase 1 deficiency attenuates cardiac dysfunction, oxidative stress, fibrosis, inflammatory via AMPK-SIRT3 pathway in diabetic cardiomyopathy mice. Int J Biol Sci. 2022;18:826–40.
40. Chen Y, Zheng Y, Chen R, Shen J, Zhang S, Gu Y, et al. Dihydromyricetin attenuates diabetic cardiomyopathy by inhibiting oxidative stress, inflammation and necroptosis via sirtuin 3 activation. Antioxidants (Basel). 2023;12:200.
41. Li Y, Wei X, Liu SL, Zhao Y, Jin S, Yang XY. Salidroside protects cardiac function in mice with diabetic cardiomyopathy via activation of mitochondrial biogenesis and SIRT3. Phytother Res. 2021;35:4579–91.
42. Wu M, Zhang C, Xie M, Zhen Y, Lai B, Liu J, et al. Compartmentally scavenging hepatic oxidants through AMPK/SIRT3-PGC1alpha axis improves mitochondrial biogenesis and glucose catabolism. Free Radic Biol Med. 2021;168:117–28.
43. Crawford K, Oliver PL, Agnew T, Hunn BHM, Ahel I. Behavioural characterisation of Macrod1 and Macrod2 knockout mice. Cells. 2021;10:368.
44. Zhan R, Meng X, Tian D, Xu J, Cui H, Yang J, et al. NAD^+ rescues aging-induced blood-brain barrier damage via the CX43-PARP1 axis. Neuron. 2023;111:3634–49.
45. Lee JH, Hussain M, Kim EW, Cheng SJ, Leung AKL, Fakouri NB, et al. Mitochondrial PARP1 regulates NAD^+-dependent poly ADP-ribosylation of mitochondrial nucleoids. Exp Mol Med. 2022;54:2135–47.